

Short Review

Effects of Aluminum Species on the Activity of NAD(P)H-dependent Dehydrogenases – a Review

Li Li², Xiaodi Yang^{1,*}, Ren Fang Shen^{3,*}, Zhaorui Pan²

¹ Jiangsu Collaborative Innovation Center of Biomedical Functional Materials, Jiangsu Key Laboratory of New Power Batteries, College of Chemistry and Materials Science, Nanjing Normal University, Nanjing 210097, China

² School of Environmental Science, Nanjing Xiaozhuang University, Nanjing 211171, China

³ State Key Laboratory of Soil and Sustainable Agriculture, Institute of Soil Science, Chinese Academy of Sciences, Nanjing 210008, China

*E-mail: yangxiaodi@njnu.edu.cn, rfshen@issas.ac.cn

Received: 27 November 2015 / Accepted: 29 March 2016 / Published: 1 April 2016

Recently, the toxicity of aluminum has attracted more attention. This review highlighted studies on the potential effects of Al(III) and nano-Al₁₃ on the activities of NAD(P)H-dependent dehydrogenases (e.g., glutamate dehydrogenase, alcohol dehydrogenase, aldehyde dehydrogenase, glutathione reductase, lactate dehydrogenase and malate dehydrogenase) at two kinds of carbon material immobilized electrodes. It revealed that Al(III) and nano-Al₁₃ could inhibit the activities of most dehydrogenases above. However, it caused an activation to that of malate dehydrogenase. We focused on the proposed interaction mechanism and discussed comprehensively at primary aspects. According to the fact, it strongly suggested that the conformational changes of coenzymes and dehydrogenases induced by Al(III) and Al₁₃ might be the main factor for the alternation of enzyme activity. Meanwhile, it also provided the detailed molecular-level information about the effects of different aluminum species to contribute to food security worldwide.

Keywords: Electrochemical method; Al(III); nano-Al₁₃; NAD(P)H-dependent dehydrogenase.

1. INTRODUCTION

There are at least six types of reactions catalyzed by NAD(P)H-dependent dehydrogenases, involving hydrogen transfer reaction, alpha-keto acid generated from amino acid, oxidation of β-hydroxyl acid and the following decarboxylation of β-keto acid, oxidation of the aldehyde, reduction of carbon-carbon double bond, oxidation of the carbon-nitrogen bond in Table 1.

Table 1. Six types of reactions catalyzing by NAD(P)H-dependent dehydrogenases

The type of reactions	The representative enzymes
$\begin{array}{c} \text{---CH---} \\ \\ \text{NH}_3^+ \end{array} \xrightleftharpoons{\text{H}_2\text{O}} \begin{array}{c} \diagup \\ \text{C} \\ \diagdown \\ \text{O} \end{array} + \text{NH}_4^+ + \text{H}^+ + 2\text{e}^-$	MDH LDH ADH
$\begin{array}{c} \text{---CH---} \\ \\ \text{NH}_3^+ \end{array} \xrightleftharpoons{\text{H}_2\text{O}} \begin{array}{c} \diagup \\ \text{C} \\ \diagdown \\ \text{O} \end{array} + \text{NH}_4^+ + \text{H}^+ + 2\text{e}^-$	GDH
$\begin{array}{c} \text{---C---CH---COO}^- \\ \quad \\ \text{OH} \quad \quad \quad \end{array} \rightleftharpoons \begin{array}{c} \diagup \\ \text{C} \\ \diagdown \\ \text{OH} \end{array} \text{---CH---COO}^- \\ \rightleftharpoons \begin{array}{c} \text{---C---CH}_2\text{---} \\ \\ \text{O} \end{array} + \text{CO}_2$	isocitrate dehydrogenase hosphogluconate dehydrogenase (PGB)
$\text{---CH=O} \xrightleftharpoons{\text{H}_2\text{O}} \text{---C=O}^- + 3\text{H}^+ + 2\text{e}^-$	ALDH
$\text{---CH---CH---} \rightleftharpoons \begin{array}{c} \diagup \\ \text{C}=\text{C} \\ \diagdown \end{array} + 2\text{H}^+ + 2\text{e}^-$	steroid reductase
$\text{---CH---NH} \rightleftharpoons \begin{array}{c} \diagup \\ \text{C}=\text{N} \\ \diagdown \end{array} + 2\text{H}^+ + 2\text{e}^-$	dihydrofolate reductase

Some NAD(P)H-dependent dehydrogenases such as glutamate dehydrogenase (GDH), alcohol dehydrogenase (ADH), malate dehydrogenase (MDH), aldehyde dehydrogenase (ALDH), glutathione reductase (GR) and Lactate dehydrogenase (LDH) are critical enzymes both in plants and animals. For example, ALDH and ADH present in the liver of humans and animals have been confirmed to be responsible for ethanol metabolism [1]. MDH has been proved to catalyze the reversible conversion between malate and oxaloacetate in the presence of NAD(H)[2]. GDH may be of particular importance not only in the plant biology, but also in the animal nerve system. LDH activity has been applied as a useful biomarker in various fields of biology, medicine, and environment [3]. GR, NADPH-dependent enzyme, distributing in bacteria, yeasts, animals and plant genomes, is the major enzyme involved in the reduction of GSSG to the important cellular antioxidant GSH in most organisms [4]. Interestingly, in our previous research, we found that Al(III) and nanometer-sized tridecameric aluminum polycation (Al₁₃) might significantly affect the activity of these NAD(P)H-dependent dehydrogenases above [5-12].

Recently, Song et al. explored that aluminum ions may induce the formation of backbone ring structures in a wide range of peptides [13]. Since Copeland and De Lima have reported that Al(III) blocked the growth of wheat roots in acidic soils [14], the toxicity of aluminum has been recognized [15,16]. Various species aluminum compounds may enter the human body by various routes, such as foods [17], water, dermal penetration, and ingestion, also may then be present in various tissues including brain [18]. More attention has been drawn to aluminum for its responsibility for some neurodegenerative diseases [19-21].

Currently, research on the potential toxicity of nanoparticles lags far behind its rapid development. It has been given rise to a debate that whether Al_{13} exist veritably in nature, but there still are some reports about Al_{13} in environment. For example, it has revealed that Al_{13} could be present in streams and lakes where water mixed with various acidity [22]. However, it has been proved that Al_{13} have 10-fold toxicities to plant root comparable to monomeric Al^{3+} [23].

In our previous systematic researches, the interactions between various forms of aluminum and NAD(P)H-dependent dehydrogenases were focused on, and the mechanism was further explained. In this paper, it reviewed and discussed the effects of Al(III) and nano- Al_{13} species on the activities of NAD(P)H-dependent dehydrogenases by electrochemical methods demonstrated in Figure 1. It showed that it could be employed in life system to evaluate the activity of biological enzyme. Moreover, the mechanism was also explored in different aspects by using fluorescence and circular dichroism (CD) spectra reflecting the conformational transformation of coenzymes and dehydrogenases.

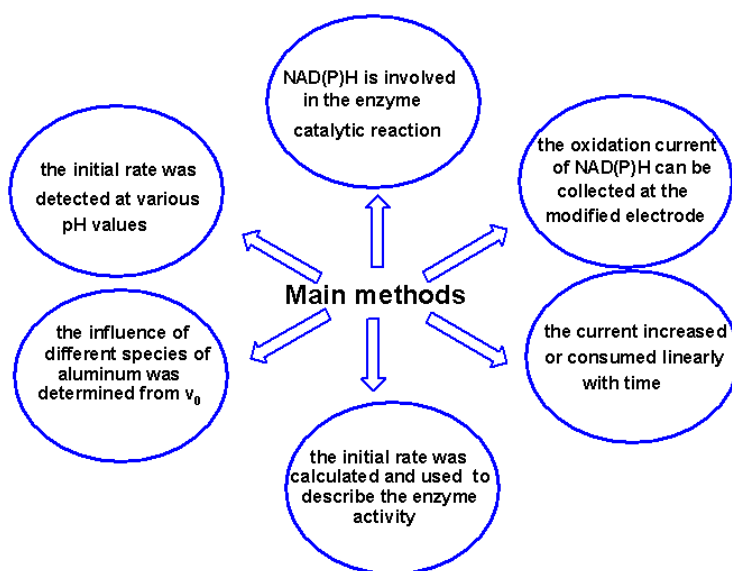


Figure 1. The main electrochemical methods involved in this paper

2. DISCUSSION

2.1 The methods of electrochemistry on novel modified electrode

It is a challenge to explore the alteration of enzyme conformation and property with the interference of additives such as metal ions and nanoparticles, because the enzymes molecular were consist of several identical subunits. Ferrer et al. have utilized Fourier transform infrared, Raman and Fluorescence spectroscopies, UV-Vis spectrophotometry, and also EPR measurements to monitor the interaction between methimazole-copper(II) and BSA[24]. Gole et al have made investigation to characterize the little perturbation to the native structure of the enzyme fungal protease utilizing FT-IR and fluorescence measurements [25]. And it also has reported that FTIR, circular dichroism and fluorescence spectroscopies were operated to indicate the conformational alteration of alcohol dehydrogenase and ketoreductase [26]. Synchrotron X-ray fluorescence and Xray absorption

spectroscopy have probed metal ions to impact the fibrinolytic activity of a homodimeric protease[27]. Further research combining Raman spectroscopy with electrochemical methods was mentioned to study lanthanide ions on the activity of MDH [28].

Electrochemical analysis was widely performed in biological system because of the superiority such as high sensitivity, quickly, lower cost, and so on. Chronoamperometric and cyclic voltammetric experiments have been applied to study the effects of lanthanide ions on the kinetics of GLDH by Zhuang et al.[29]. The hanging mercury drop electrode (HMDE) and bare glassy carbon electrode were also attempted to measure LDH activity, respectively [7, 30]. However, because of the toxicity, the application of mercury drop electrode was limited. Though the carbon nanotubes may be employed *in vivo*, the van der Waals between the tube walls will lead to aggregate, which goes against the modification of electrode. Reduced graphene has been proved to catalyze the redox reactions excellent in supercapacitors, lithium batteries and electrochromic devices [31].

In this paper, the prepared electrode was obtained as follows. The dried GCE surface was coated with GO/CHIT solution, and then was reduced by hydrazine at 70 °C, thus, the rGO/CHIT modified electrode was finished.

2.1.1 The electrochemical response of NAD(P)H on two carbon material modified electrodes

The cyclic voltammetry (CV) of the oxidation of NAD(P)H showed the properties of the modified electrodes in Figure 2. The significant electrocatalytic behavior of the proposed electrode was observed by the substantial negative shift of the anodic peak. The peak potential of NAD(P)H oxidation is in the 550-850 mV range on the bare electrode, whereas, many distracters such as catecholamine, ascorbic acid and urea are present [32].

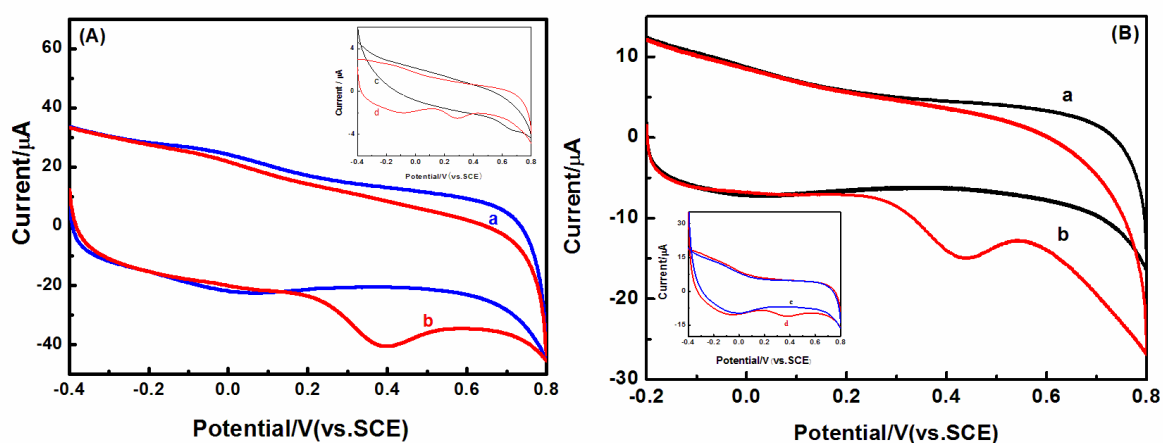


Figure 2. (A) Cyclic voltammograms of the oxidation of NADH on (a) and (c) bare electrode; (b) rGO fixed electrode in 5 mL pH 7.0 Tris-HCl buffer solution containing 1.5 mM NADH. Scan rate: 10 mV/s. (B) CV of NADPH on (a) and (c) bare electrode; (b) rGO fixed electrode in 5 mL pH 7.5 Tris-HCl buffer solution containing 1.0 mM NADPH. Scan rate: 10 mV/s. (Reproduced from the permission from [12]. Copyright 2012 Chinese Journal of Analytical Chemistry)

At both carbon material fixed electrodes, the oxidation peak potential decreased successfully and the peak current was also improved evidently [6,12]. The negative shift of the anodic peak demonstrated that both materials made the electron transfer easier to reveal catalytic properties. Moreover, from the intensity of peak current, it can be concluded that the performance of rGO fixed electrode is superior to that of MWNT. Finally, the fixed electrode was measuring the acceptable reproducibility and remaining approximately 95% of the initial current response. These data implied that the surface fouling was fully eliminated and the perfect performance of immobilized electrodes was exhibited.

The amperometric response ($i-t$) was collected at regular interval injection of NAD(P)H in Figure 3. It presents a linear range at two carbon material fixed electrodes [6, 11, 12]. So the proposed electrodes could be adopt to monitor the electrochemical signal change of NADH generated or NADPH consumed in the enzymatic reaction.

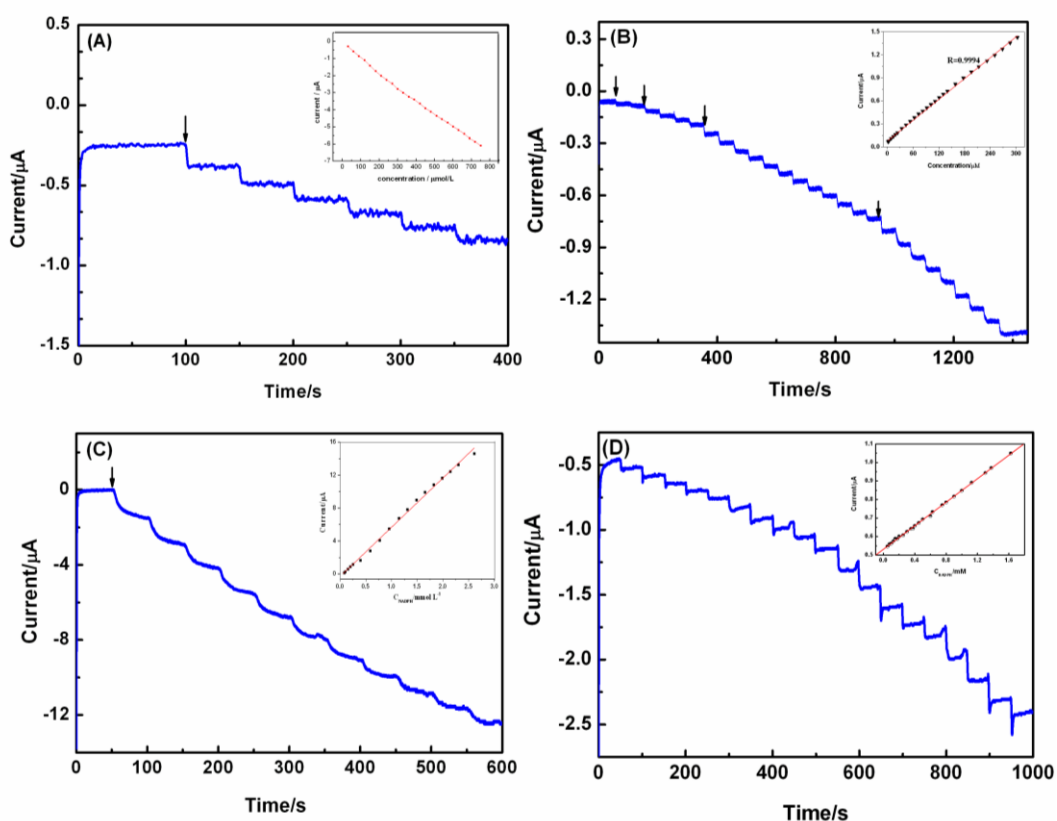


Figure 3. Amperometric $i-t$ curves of the NADH at (A) Reproduced from the permission from [11]. Copyright 2011 Sensors) MWNT fixed electrode and (B) (Reproduced from the permission from [6]. Copyright 2013 IEEE) rGO fixed electrode in pH 7.0 Tris-HCl buffer solution, and amperometric response of NADPH on (C) (Reproduced from the permission from [12]. Copyright 2012 Chinese Journal of Analytical Chemistry) MWNT fixed electrode and (D) rGO fixed electrode in pH 7.0 Tris-HCl buffer solution. Each time is the interval of 50s. (The insert represent the linear relationship between the concentration of coenzyme and the amperometric response.)

2.1.3 The application of chronoamperometry on determination of dehydrogenase activity

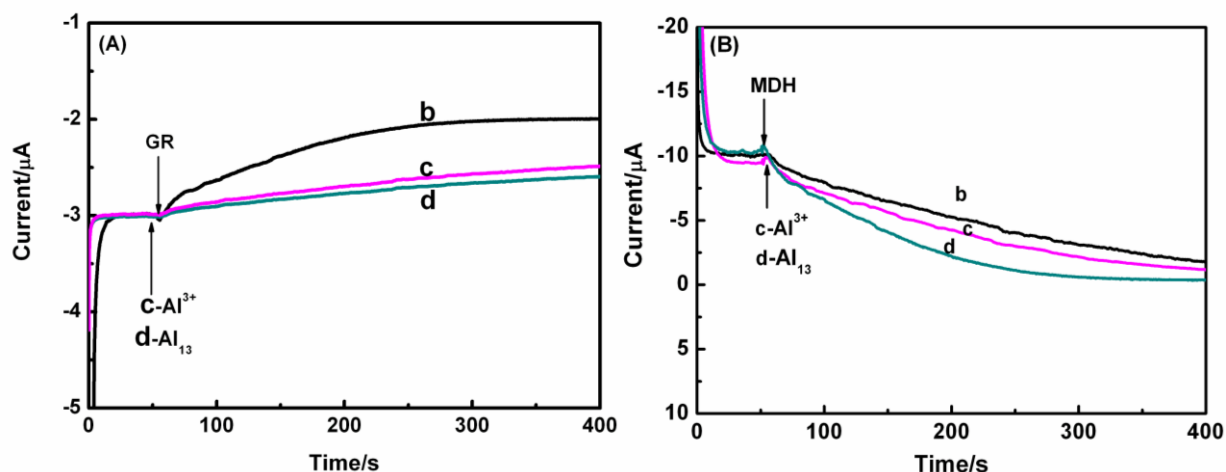


Figure 4. (A) Amperometric response of NADPH at MWNT modified electrode: (b) without Al³⁺ and Al₁₃; (c) 50 μM Al³⁺; (d) 50 μM Al₁₃; (Reproduced from the permission from [12]. Copyright 2012 Chinese Journal of Analytical Chemistry) (B) Amperometric response of NADH at MWNT modified electrode: (b) without Al³⁺ and Al₁₃; (c) 30 μM Al³⁺; (d) 30 μM Al₁₃ (Reproduced from the permission from [11]. Copyright 2011 Sensors)

As we know, in the enzymatic catalytic reaction, during the first seconds at the beginning of catalyzed reaction, the current is increasing or consuming linearly with time. That is to say, the amount of NADH newly generated or NADPH consumed could be calculated accurately, thus, the initial rate (v_0) could be confirmed according to the curve gradient, which may determine the validity of the enzyme. The influences of Al(III) and Al₁₃ on the v_0 could be seen obviously in Figure 4.

The analytical performance of the proposed immobilized electrode was tested by collecting the $i-t$ curves for the oxidation of NAD(P)H. In general, it was clear that with the addition of the dehydrogenase, the anodic oxidative current of NAD(P)H dramatically improved, which mean that the dehydrogenase indeed catalyzed the reaction. In these two systems, it displayed the opposite trends of the gradient of the curves (b~d) with the addition of aluminum. For instance, in Figure 4A, when adding Al(III) and nano-Al₁₃ to the system, the slope of curves c and d became smaller, which indicated that the rate of enzyme-catalyzed reaction was slow down, thus Al(III) and Al₁₃ display inhibition to GR activity [12]. However, in Figure 4B, compared with curve b, curves c and d are sharper, which demonstrated that the Al(III) and Al₁₃ accelerated the enzyme-catalyzed reaction and activated the MDH activity [11]. The results obtained deduced that Al(III) and Al₁₃ could slow down the activity of GR, conversely, activate that of MDH.

Therefore, it revealed that the amperometric $i-t$ measurement could accurately determine the activity of the dehydrogenase by tracing the increase or consumption of oxidation current of NAD(P)H. Moreover, it could be concluded that nano-Al₁₃ showed the stronger effect than that of Al(III) to the activity of dehydrogenases in all cases.

2.2 The dehydrogenase activity in the present of Al^{3+} and Al_{13}

In the progress of enzymatic reaction, it was found that there was positive linear relationship between the current of NAD(P)H and time within the first few minutes. According to that, v_0 could be calculated to monitor the enzyme activity. In our previous study, various species aluminum exhibited the same inhibition to the feature of most dehydrogenases in the catalytic reaction. However, it surprisingly stimulated the catalytic performance of MDH, and the results were similar with other researches [33]. The effects of Al(III) and Al_{13} on the validity of NAD(P)H-dependent dehydrogenases were explored successfully by the amperometric curves, which were listed in Table 2.

Table 2. The effects of Al(III) and nano- Al_{13} on the activity of NAD(P)H-dependent dehydrogenase

Enzymes	Electrochemical Methods	Al species effects		Reference
		Al (III)	Al_{13}	
GDH	Testing the differential-pulse polarography (DPP) reduction current and CV of NAD^+ at the HMDE-SCE	At pH of 6.5 and 7.5, the GDH activities were remarkable depended on the concentrations of the metal ion added.		[10]
	Monitoring the CV and <i>i</i> -t curves of NADH at the MWNT-GCE	Al^{3+} showed the strongest inhibitory at pH 6.5, while effects deduced with the increasing of pH value.	The level of inhibiting effects of Al_{13} was the highest at pH 7.5, and it showed the similar inhibition at pH 6.5 and 8.5.	[5]
GR	Monitoring the CV and <i>i</i> -t curves of NADPH at the MWNT-GCE and rGO-GCE	Al^{3+} showed the inhibition, while there was a minimum effect of Al^{3+} concentration at every pH value.	Al_{13} inhibited the GR activity, and there was a maximum effect at pH value of 7.4.	[12]
ADH	Monitoring the CV and <i>i</i> -t curves of NADH at the MWNT-GCE and rGO-GCE	The activity was strongly inhibited at pH 6.5, and the effect was gradually weaker with the increasing of pH value.	Al_{13} showed the strongest effect on the activity of ADH at pH 7.5, and the similar inhibition effect at pH value of 6.5 and 8.5.	[9]
MDH	Monitoring the CV and <i>i</i> -t curves of NADH at the MWNT-GCE	Al(III) showed the strongest activated effect on the activity of MDH at pH 6.5. At pH 6.5 and 8.5, the activated effect	Al_{13} showed the strongest activated effect on the activity of MDH at pH 7.5. The activated effect will reach the maximum	[11]

		will reach the maximum level, while the maximum point varied with different pH values (6.5 to 8.5)	level, while the maximum point varied with different pH values (6.5 to 8.5).	
ALDH	Monitoring the CV and <i>i</i> -t curves of NADH at the rGO fixed electrode	The addition of Al(III) apparently inhibited the ALDH activity at pH 6.0.	The effect of Al ₁₃ was the highest at Ph 7.0, and it displayed the similar inhibition effect at pH 6.0 and 8.0.	[6]
LDH	Detecting the current of NAD ⁺ at HMDE by DPV curves	It showed that the trend of the effect of Al(III) was different at various pH values. When the pH value lean to alkaline, LDH activity showed a trend to increase; but when the pH value lean to acidity, it showed inhibitory effects.	It indicated that the inhibitory effects were observed at three pH values of 6.5, 7.5 and 9.2	[8]

2.3 The explanation of the mechanism of the interaction between aluminum and dehydrogenases

2.3.1 The ability of aluminum binding to the substrates

We estimated the binding ability of aluminum to substrates from the aluminum-ligands binding constants in aqueous solution as shown in Table 3.

Table 3. The stability constants of various aluminum-substrates complexes

	α -KG	L-Glu	Lactic acid	Malic acid	NAD ⁺	NADP ⁺
logK(HL)			3.61			9.93
logK(H ₂ L)	2.41	2.17		4.45	3.46	16.09
logK(HL ⁻)	4.63	3.98		3.15	10.95	19.90
logK(L ²⁻)		8.96				
log β (AlLH ₂ ³⁺)					15.60	19.16
log β (AlLH ²⁺)	6.55	10.68			12.31	16.01
log β (AlL ⁺)	3.83	7.42	2.36	3.32		10.71
log β (AlLH _{.1})	-0.87	2.56				

$\log\beta(\text{AlL}_2)$	5.75	4.42	
$\log\beta(\text{AlL}_2\text{H}_2^{3-})$	-5.48		
$\log\beta(\text{Al}_2\text{L}_2^{2+})$			19.82
$\log\beta(\text{AlL}^+)$	6.32	9.56	
$\log\beta(\text{AlLH}_1)$		5.80	

It could be seen that the reaction substrates in the NAD(P)H-dependent dehydrogenase system were rather weaker when binding with aluminum. The binding ability of these bioligands was similar to that of common dicarboxylic acid. Therefore, transformation of the constitution and configuration for these bioligands were not the major reason for the NAD(P)H-dependent dehydrogenase activity alternation at physiological condition. However, it clearly showed that the binding constants of Al-NAD^+ were larger than these substrates, so we predicted that the configuration change of NAD^+ induced by binding with NAD^+ might be one of the major reason.

2.3.2 The effects of aluminum on the conformation of the coenzyme

When added to the system, aluminum complexed with the active site may lead to the change of NAD^+ conformation, which resisted the recognition of substrate by enzyme. The fluorescence spectra uncovered that Al(III) and Al_{13} might result in the conformation of NAD^+ from the open to the folded form [5]. It was known that the folded structure of NAD^+ might be precise determined by fluorescence spectrum. In Figure 5, with the increase of the Al(III) and Al_{13} concentration, the increase of fluorescence intensity could be attributed to the structural changes of NAD^+ from open form to folded form.

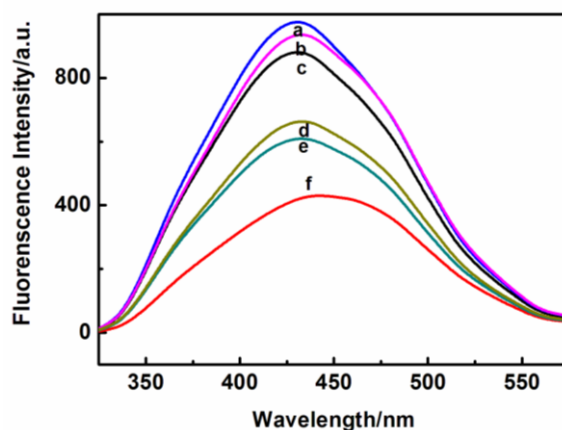


Figure 5. Fluorescence spectra of NAD^+ with increasing aluminum concentration. ($C_{\text{NAD}^+}=10\mu\text{M}$, curves a-c are present with $L/\text{Al}_{13}=1:4, 1:1, 1:1/4$ respectively; curves d-f are present with $L/\text{Al}^{3+}=1:4, 1:1, 1:0$) (Reproduced from the permission from [5]. Copyright 2010 Elsevier)

2.3.3 The effects of aluminum on the conformation of the NAD(P)H-dependent hydrogenases

The activity of dehydrogenase was closely related to its structure. Therefore, the conformational change of dehydrogenase induced by the influence of aluminum would affect the induced-fit between enzyme and substrates, which contributed to the enzyme activity. In Figure 6, with the addition of aluminum, a decrease in α -helices and β -sheets with an increase in random coil were displayed in CD spectra, [34], which signified the conformation change to unfavorable structure of ALDH, ADH, MDH and GR. In the far-UV region, the typical spectrogram of α - helices structure of protein was shown as the split-hump [35].

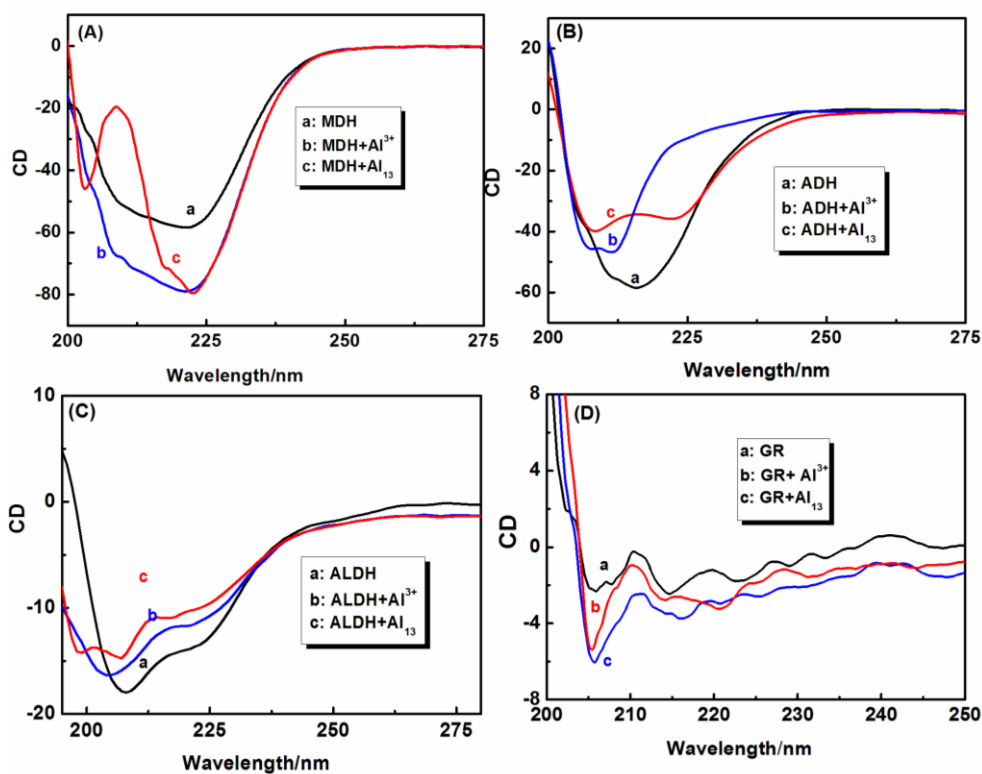


Figure 6. CD spectra of (A) MDH; (Reproduced from the permission from [11]. Copyright 2011 Sensors) (B) ADH; (C) ALDH (Reproduced from the permission from [6]. Copyright 2013 IEEE) and (D) GR with and without addition of Al(III) and Al₁₃. (Reproduced from the permission from [12]. Copyright 2012 Chinese Journal of Analytical Chemistry)

The feature in the far-UV region determined that nano-Al₁₃ could increase the amount of α -helices structure of MDH [11], which might make the substrate more easily access to the surface active site to achieve the induced-fit. Similarly, the CD spectral of ADH, ALDH and GR had undergone a remarkable change when adding Al(III) and Al₁₃ to the systems [6,12]. We could observe another distinct changes in the CD spectra of ADH with addition of Al(III) and Al₁₃, which showed the alternation in the secondary structure of the enzyme. However, except MDH, the structure change of ADH, ALDH and GR might lead to an unsatisfactory configuration to induced-fit, which decreased the enzyme activity.

The inhibition of Al(III) and nano-Al₁₃ to dehydrogenase might be recognized from electronic structure. For example, in the simulation of ALDH consisting of two identical units [36], NAD⁺ is combined with CYS243 when ALDH catalyzes ethanol to acetaldehyde. However, when added Al(III) or nano-Al₁₃ to the mixture, aluminum competed to occupy the active binding sites on the surface, which led to the change of the ratio of the open and folded conformation of NAD⁺. And this may be the main reason for the decrease of ALDH validity.

In previous researches, various Al speciations always slow down the enzyme activity. However, it accelerated MDH activity. Therefore it was significant to discuss the proposal explanation. The influence of Al(III) and Al₁₃ to MDH may be considered as follows.

The mechanism also can be comprehended by the formation of an enzyme-substrate-coenzyme complex. While the enzyme oriented the reactants relative to each other, first step occurred between the reactants and enzyme surface in the catalyzed reaction. Then, the enzyme opened up to release the product after the catalysis finished. This step may be the critical stage in the whole reaction. In the progress of this catalytic reaction, oxaloacetic acid was oxidized to malic acid with NADH transformed to NAD⁺. So the disaggregation of NAD⁺-MDH complex was the rate-limiting step. As it has been reported that Al(III) and Al₁₃ could complex with the adenine N₇ and free oxygen of pyrophosphate groups in NAD⁺ structure [37]. We reasonable predicted that aluminum preferred to combine with NAD⁺, which could speed up the disaggregation of the NAD⁺-MDH. That is to say, the combination of aluminum and NAD⁺ was responsible for the acceleration of aluminum to MDH.

3. CONCLUSION

In this paper, the effects of Al(III) and nano-Al₁₃ on the activity of NAD(P)H-dependent dehydrogenase were successfully introduced, on the functionalized MWNT-GCE and rGO-GCE modified electrodes. It indicated that not all aluminum species displayed the similar toxicity, and the nano-Al₁₃ testified the stronger effect. In the meantime, amperometric *i-t* measurement also may be performed as an efficient way for monitoring enzyme activity. The conformational changes of NAD⁺ and dehydrogenase had been discovered definitely with assistance by the fluorescence technique and CD spectra, and it was predicted that the transformation of conformation for NAD⁺ and dehydrogenase might be responsible for the alternation of validity.

ACKNOWLEDGEMENTS

The project is supported by the National Natural Science Foundations of China (21575067, 21301094), the research funding of Jiangsu Administration of Environment Protection (2015020), State Key Laboratory of Analytical Chemistry for Life Science (SKLACLS1308) and Nanjing Xiaozhuang University (2015NXY36). We also thank for Research Funding from the State Key Laboratory of Soil and Sustainable Agriculture (0812201216).

References

1. S. L. Lee, G. Y. Chau, C. T. Yao, C. W. Wu and S. J. Yin, *Alcohol. Clin. Exp. Res.*, 30 (2006) 1132
2. C. R. Goward, D. J. Nicholls, *Protein Sci.*, 3 (1994) 1883
3. A. D. Ellington, J. J. Bull, *Science*, 310 (2005) 454

4. L. Marty, S. Wafi, M. Schwarzlander, M. D. Fricker, M. Wirtza, L. J. Sweetlove, Y. Meyer, A.J. Meyer, J.P. Reichheld and H. Rudiger, *PNAS.*, 106 (2009) 9109
5. L. Cai, X.F. Xie, L. Li, H.H. Li, X.D. Yang and S. Q. Liu, *Colloid. Surface B.*, 81 (2010) 123
6. L. Li, N.N. Zhang, X. L. Ma, C. Z. Xu, H.Y. Wei, X. J. Yang and X. D. Yang, *IEEE Sens. J.*, 13 (2013) 314
7. K. A. Yao, N. Wang, J. Y. Zhuang, Z. B. Yang, H. Y. Ni, Q. Xu, C. Sun, and S. P. Bi, *Talanta*, 73 (2007) 529
8. N. Wang, D. Q. Huang, J. Zhang, J. J. Cheng, T. Yu, H. Q. Zhang and S. P. Bi, *J. Chem. Phys.*, 112 (2008) 18034
9. X. L. Wang, L. Li, Y. P. Wang, C. Z. Xu, B. Zhao and X. D. Yang, *Food Chem.*, 138 (2013) 2195
10. X. D. Yang, L. F. Li and S. P. Bi, *Sensors*, 5 (2005) 235
11. X. D. Yang, L. Cai, Y. Peng, H. H. Li, R. F. Chen and R. F. Shen, *Sensors*, 11(2011) 5740
12. N. N. Zhang, Y. Z. Tang, F. Ma, H. H. Li, T.H. Lu and X. D. Yang, *Chinese J. Anal. Chem.*, 40 (2012) 584
13. B. Song, Q. Sun, H. K. Li, B. S. Ge, J. S. Pan, T. S. Wee Andrew, Y. Zhang, S. H. Huang, R. H. Zhou, X. Y. Gao, F. Huang and H. P. Fang, *Angew. Chem. Int. Edit.*, 53 (2014) 6358
14. L. Copeland, M.L. De Lima, *J. Plant. Physiol.*, 140 (1992) 641
15. E. Delhaize, B. D. Gruber and P. R. Ryan, *FEBS Lett.*, 581 (2007) 2255
16. T. Ikka, T. Ogawa, D. H. Li, S. Hiradate and A. Morita, *Phytochemistry*, 94 (2013) 142
17. C. F. Struller, P. J. Kelly and N. J. Copeland, *Surf. Coat. Tech.*, 241(2014) 130
18. T. T. Win-Shwe and H. Fujimaki, *Int. J. Mol. Sci.*, 12 (2011) 6267
19. S. C. Bondy, *Toxicology*, 315 (2014) 1
20. N. Cabus, E. O. Oguz, A.C. Tufan and E. Adiguzel, *Biotech. Histochem.*, 90 (2015) 132
21. A. N. Hashmi, A. Yaqinuddin and T. Ahmed, *Int. J. Neurosci.*, 125 (2015) 277.
22. L. Parent and P. G. C. Campbell, *Environ. Toxicol. Chem.*, 13 (1994) 587
23. G. Furrer, B. L. Phillips, K. U. Ulrich, R. Pothing and W. H. Casey, *Science*, 297 (2002) 2245
24. N. M. Urquiza, L. G. Naso, S. G. Manca, L. Lezama, T. Rojo, P. A. M. Williams and E. G. Ferrer, *Polyhedron*, 31 (2012) 530.
25. A. Gole, C. Dash, A. B. Mandale, M. Rao and M. Sastry, *Anal. Chem.*, 72 (2000) 4301.
26. G. A. Petkova, K. Zaruba and V. Kral, *Biochim. Biophys. Acta*, 1824 (2012) 792.
27. J. Siritapetawee, W. Limphirat, C. Kantachot and C. Kongmark, *Appl. Biochem. Biotechnol.*, 175 (2015) 232
28. Q. K. Zhuang, H. C. Dai, *J. Electroanal. Chem.*, 499 (2001) 24
29. Q. K. Zhuang, H. C. Dai, X. X. Gao and W. K. Xin, *Bioelectrochemistry*, 52 (2000) 37
30. Z. H. Gan, Q. K. Zhuang, J. X. Zhang, *Chin. J. Anal. Chem.*, 30 (2002) 385
31. Y. Z. Tang, C. Sun, X. J. Yang, X. D. Yang and R. F. Shen. *Int. J. Electrochem. Sci.*, 8 (2013) 4194
32. A. Sobczak, T. Rebis and G. Milczarek, *Bioelectrochemistry*, 106 (2015) 308
33. C. Wang, X. Q. Zhao, M. Sunairi, T. Aizawa and R. F. Shen, *Pedosphere*, 23 (2013) 29
34. F. Ma, C. Sun, W. S. Zhou, C. Z. Xu, J. H. Zhou, G. X. Wang and X. D. Yang, *Spectrochim. Acta, Part A.*, 97 (2012) 885
35. N. Greenfield and G. D. Fasman, *Biochemistry*, 8 (1969) 4108
36. Z. J. Liu, Y. J. Sun, J. Rose, Y. J. Chung, C. D. Hsaio and W R. Chang, *Nat. Struct. Biol.*, 4 (1997) 317
37. X. D. Yang, S. P. Bi, L. Yang, Y. H. Zhu and X. L. Wang, *Spectrochimica Acta Part A*, 59 (2003) 2561